JOURNAL OF RHEOLOGY

Scaling laws for the slumping of a Bingham plastic fluid

Lydie Staron, Pierre-Yves Lagrée, Pascal Ray, and Stéphane Popinet

Citation: J. Rheol. **57**, 1265 (2013); doi: 10.1122/1.4802052
View online: http://dx.doi.org/10.1122/1.4802052
View Table of Contents: http://www.journalofrheology.org/resource/1/JORHD2/v57/i4
Published by the The Society of Rheology

Related Articles

Concentration fluctuations in polymer solutions under extensional flow
J. Rheol. 57, 1211 (2013)

The matching of a “one-dimensional” numerical simulation and experiment results for low viscosity Newtonian and non-Newtonian fluids during fast filament stretching and subsequent break-up
J. Rheol. 56, 159 (2012)

Hard vs soft constraints in the full field reconstruction of incompressible flow kinematics from noisy scattered velocimetry data
J. Rheol. 55, 1187 (2011)

Shear and extensional rheology of polypropylene melts: Experimental and modeling studies
J. Rheol. 55, 95 (2011)

Molecularly derived constitutive equation for low-molecular polymer melts from thermodynamically guided simulation
J. Rheol. 55, 69 (2011)

Additional information on J. Rheol.

Journal Homepage: http://www.journalofrheology.org/
Journal Information: http://www.journalofrheology.org/about
Top downloads: http://www.journalofrheology.org/most_downloaded
Information for Authors: http://www.journalofrheology.org/author_information

ADVERTISEMENT

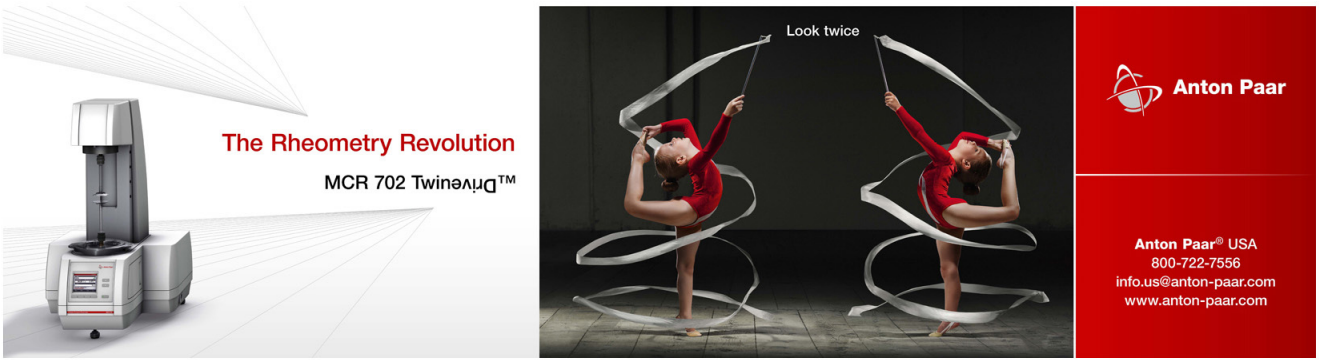

Scaling laws for the slumping of a Bingham plastic fluid

Lydie Staron[a)]

CNRS–Université Pierre et Marie Curie Paris 6, UMR 7190, Institut Le Rond d'Alembert, F-75252 Paris, France and School of Earth Sciences, University of Bristol, Queens Road, Bristol BR8 1RJ, United Kingdom

Pierre-Yves Lagrée and Pascal Ray

CNRS–Université Pierre et Marie Curie Paris 6, UMR 7190, Institut Jean Le Rond d'Alembert, F-75252 Paris, France

Stéphane Popinet

National Institute of Water and Atmospheric Research, P.O. Box 14-901 Kilbirnie, Wellington, New Zealand

(Received 30 May 2012; final revision received 27 March 2013; published 26 June 2013)

Synopsis

Bingham plastics exhibit complex behaviors, depending on both geometrical and rheological factors, and are difficult to characterize systematically. This is particularly true in the case of transient flows, where solidlike and fluidlike behaviors coexist in an intermittent fashion. The aim of this contribution is to study the slump of Bingham columns under gravity, while varying systematically and independently both the geometry of the system and the rheological parameters. To do so, numerical experiments are carried out in two dimensions with a non-Newtonian Navier–Stokes code, the Gerris flow solver, using a volume-of-fluid approach. We are able to determine the slump height and the spreading of the column after motion ceased. These characteristics are related to the rheological properties and initial shape through scaling relationships. The results are compared with previous scalings and prediction from the literature. A discussion ensues on the importance of the normalization choice and of unambiguous discrimination between geometrical and material factors. © *2013 The Society of Rheology*. [http://dx.doi.org/10.1122/1.4802052]

I. INTRODUCTION

The flow of yield stress materials under gravity is encountered in many situations of industrial, engineering, and geophysical relevance. Mud and slurries, as those dealt with not only in off-shore construction but also in mining processes and in the agro- and food-industries (fertilizers, emulsified food, etc.), show a typical yield behavior: A minimum stress must be applied for the material to start flowing. Fresh concrete, whose rheological

[a)]Author to whom correspondence should be addressed; electronic mail: lydie.staron@upmc.fr

properties are crucial for those using it, is a well-known example of yield stress material [Ferraris and de Larrard (1998); Schowalter and Christensen (1998); Roussel *et al.* (2005)]. In a different context, lahars resulting from heavy rainfalls in volcanic areas show similar flow properties [Whipple (1997); Tallarico and Dragoni (2000)]. The slow failure of muddy soils is another dramatic manifestation of yield behavior.

Despite their apparent diversity, in a first approximation, all these materials can be described as Bingham plastics in a large number of situations: They behave like solids at low stress and flow like viscous fluids at high stress. In this simplified picture, a yield stress and a viscosity define them nearly completely. However, in the face of the simplicity of the mathematical form of Bingham's model, Bingham plastics exhibit a complex behavior difficult to characterize systematically. This is particularly true in the case of transient flows, where solidlike and fluidlike behaviors coexist in an intermittent fashion. Because the existence of a yield stress implies the existence of an intrinsic length scale (given by the ratio of the yield stress to the density times gravity $L_y = \tau_y/\rho g$), the geometry of the system will play a role. In the case of gravity induced flows, the height of the system will command whether the system can flow or not [Roussel and Coussot (2005)]. This geometrical constraint is not easy to deal with. In spite of its fundamental role in the subsequent flow [Sader and Davidson (2005)], previous works on slump test for concrete do not offer an unambiguous characterization of the role of rheology and geometry independently one from the other [Pashias *et al.* (1996); Ferraris and de Larrard (1998); Schowalter and Christensen (1998); Roussel and Coussot (2005)]. Extensive theoretical work on the slumping of viscoplastic material was achieved; however, it is mostly valid in the framework of long-wave approximation, that is for squat systems [Balmforth *et al.* (2007); Dubash *et al.* (2009); Hogg and Matson (2009)]. Predictions using limit analysis for cylinders and rectangles of yield stress material can be made for incipient failure conditions [Chamberlain *et al.* (2004)]. Yet, the complex interplay of geometry and rheology in the gravity flow of Bingham systems still needs clarification. Because high values of the yield stress imply small lateral deformation, it is often assumed that plastic viscosity plays no role in the final shape of the slumping system [Sader and Davidson (2005); Roussel and Coussot (2005)]. In the case of low yield stress, however, lateral spreading becomes important, hence shear deformation, and viscous stresses are likely to affect the overall deformation. Again, the specific role of the plastic viscosity may depend on the initial geometry of the system.

The aim of this contribution is to study the slump of two-dimensional (2D) Bingham columns under gravity, while varying systematically and independently both the initial geometry of the system and the two rheological parameters: Yield stress and plastic viscosity. To do so, numerical experiments were carried out in 2D with a non-Newtonian Navier–Stokes code, the Gerris flow solver, using a volume of fluid (VOF) approach [Popinet (2003); Sader and Davidson (2005); Lagrée *et al.* (2011)]. Determining the slump height and the spreading of the column after motion ceased, we relate these characteristics to rheological properties and initial shape and try to disclose "universal" scaling relationships. The results are compared with previous scaling and prediction from the literature [Sader and Davidson (2005); Pashias *et al.* (1996)]. A discussion ensues on the importance of the normalization choice and the importance of unambiguous discrimination between geometrical and material factors.

II. NUMERICAL MODEL AND SIMULATIONS

The slumping test consists of allowing a column of material to collapse and spread under gravity onto a horizontal plane, as shown in Fig. 2 (half-column shown with a symmetry condition). This well-constrained system in terms of both rheology and geometry

is of academic interest, and furthermore, is of practical relevance to *in situ* rheological tests for concrete (the Abrams cone test, for instance) or for the failure of geological material. In practical applications—for instance, when testing fresh concrete using slumping tests—the column obeys an axisymmetric geometry; for the sake of simplicity, however, we consider in the present study a real 2D geometry, but will nevertheless refer to the lateral dimension of the system as *radius*.

A. The Gerris flow solver: A two-phase description

The simulations were performed using the (open source) Gerris flow solver in two dimensions. Gerris solves the Navier–Stokes equation for a biphasic mixture using a volume-of-fluid approach [Scardovelli and Zaleski (1999); Popinet (2003)]. The existence of two fluids translates numerically in different properties (viscosity and density) on the simulation grid following the advection of the volume fraction representing the proportion of each fluid. In our case, one fluid stands for Bingham plastic (characterized by a yield stress and a plastic viscosity) and the other stands for the surrounding air (with a low density and low viscosity); the position of the interface between the two is solved in the course of time based on the spatial distribution of their volume fraction. This method is in its main features identical to that applied by Davidson *et al.* (2000) and Sader and Davidson (2005) for the gravity flow of viscoplastic material.

In Lagrée *et al.* (2011), we show that choosing for the surrounding fluid (or "air"), a viscosity and a density 100 times smaller than that of the non-Newtonian fluid studied does not affect the dynamics of the latter, based on systematic comparison with an analytical solution. Accordingly, in this contribution, we choose for the surrounding fluid, a viscosity and a density 100 times smaller than that of the Bingham fluid. The viscosity of the Bingham fluid is constant at large shear and diverges at low shear. Using a simple regularization technique, we implement the viscosity as follows:

$$\eta_{Bingham} = \min\left(\frac{\tau_y}{D_2} + \eta\,;\, \eta_{\max}\right), \tag{1}$$

where τ_y is the yield stress, η is the plastic viscosity, and D_2 is given by the second invariant of the strain rate tensor $\boldsymbol{D}$: $D_2 = \sqrt{2D_{ij}D_{ij}}$. Numerically, the divergence of the viscosity is bounded by a maximum value η_{max} set to 10^4–10^5 times the value of η; we have checked that the choice of η_{max} does not affect the results as long as η_{max}/η is large enough (down to 10^2 in the configuration studied here). Following this formulation, we see that the plastic viscosity η plays a role only in the limit of sufficiently high deformation; for large values of the yield stress τ_y, its influence is expected to become marginal, justifying the choice of setting its value to zero [Sader and Davidson (2005); Roussel and Coussot (2005)] or ignoring its influence [Pashias *et al.* (1996); Schowalter and Christensen (1998)]. In this contribution, however, we show that the influence of the plastic viscosity η in the sideways spreading, when the latter occurs, is always apparent.

A no-slip boundary condition is imposed at the base of the flow, and a symmetry condition is imposed at the left wall. The Gerris flow solver uses an adaptive mesh refinement as shown in Fig. 1, thus limiting computational costs. No experimental data were available to test the results of the numerical simulations of Bingham fluid; however, it was successfully tested against analytical solution for cylindrical Couette flow [Bird *et al.* (1987)] as part of the Gerris test suite.[1] Moreover, the Gerris solver was used to

[1] http://gerris.dalembert.upmc.fr/gerris/tests/tests/couette.html

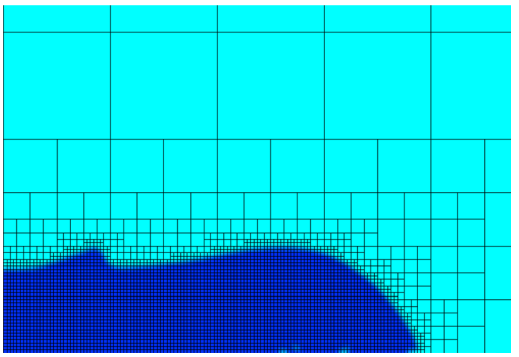

FIG. 1. Adaptive mesh refinement during the simulation of a slump using the Gerris flow solver.

reproduce the gravity flows of granular media as non-Newtonian viscous fluid, and led to the successful recovery of experimental results in different configurations, including the silo [Staron *et al.* (2012)], and more relevantly to the present work, the collapse of 2D columns under gravity [Lagrée *et al.* (2011)]. The reader is referred to Popinet (2003, 2009) for a comprehensive presentation of the Gerris Navier–Stokes solver.

B. The slumping test: Geometrical and rheological parameters

The initial geometry is characterized by the initial (real 2D) radius R_0 and initial height H_0; the initial aspect ratio is denoted $a = H_0/R_0$ (Fig. 2). In order to investigate the effect of geometrical factors on the slumping, both the radius R_0 and the initial height H_0 were alternatively varied. Accordingly, the aspect ratio varies between 0.2 and 19.

The final state is characterized by the final spread—or run-out—R and the final height H, the slump being defined as the difference between the initial and the final height $H_0 - H$. In the course of time, the position of the front is denoted r and the position of the top of the collapsing column in contact with the left boundary is denoted h. In practice, r and R are given by the maximum lateral excursion of the domain occupied by Bingham material, and h and H by the maximum excursion of the Bingham material at

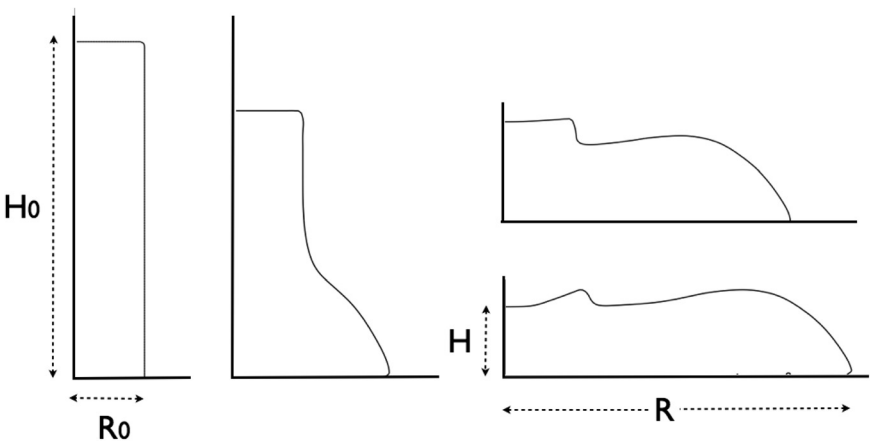

FIG. 2. Snapshots of the slumping of a half-column of Bingham plastic simulated with Gerris, with initial aspect ratio $a = H_0/R_0 = 5$, yield stress $\tau_y/\rho g R_0 = 0.33$, and plastic viscosity $\eta/\rho g^{1/2} R_0^{3/2} = 0.86$, at times $t/\sqrt{H_0/g} = 0$, 0.85, 1.70, and in the final state.

the left-hand side boundary of the simulation domain. The transition between the Bingham material and the surrounding air being sharp (over 2–3 cells), the error when evaluating R and H is about 2%–5% (error bars are not shown on the graphs).

The rheological properties of the material were systematically varied. Because the initial height H_0 sets the value of the initial compressional stress, to be compared with the characteristic yield length scale $L_y = \tau_y/\rho g$, we choose to use the initial width R_0 to normalize the rheological parameters in order to allow unambiguous discrimination between material and geometrical factors. The effect of the initial height H_0 is singled out using the purely geometrical parameter $a = H_0/R_0$.

The yield stress τ_y was set so that the normalized yield stress $\bar{\tau}_y = \tau_y/\rho g R_0$ varies between 0.06 and 1.6. Since $a = H_0/R_0$ varies between 0.2 and 19, the simulations cover the two following cases: $H_0/L_y \ll 1$, for which we expect no or little motion to occur, and $H_0/L_y \gg 1$, for which large motion is expected. The value of the plastic viscosity η was set so that $\bar{\eta} = \eta/\rho g^{1/2} R_0^{3/2}$ varies between 10^{-2} and 5. Figure 3 shows all the combined values of normalized yield stress and plastic viscosity used for this study; each point on the graph corresponds to a series of simulations with aspect ratio a varying from 0.2 to 19. For comparison, fresh concrete exhibits a yield stress ranging typically from 0.012 to $0.076 \times \rho g L$, and a plastic viscosity typically between 3×10^{-2} and $6 \times 10^{-2} \times \rho g^{1/2} L^{3/2}$, where $\rho \simeq 2500\,\mathrm{kg\,m^{-3}}$, $g = 9.81\,\mathrm{m\,s^{-2}}$, and $L = 1\,\mathrm{m}$ [data taken from Dufour and Pijaudier-Cabot (2005)]. For toothpaste, a typical value for the yield stress is $0.017 \times \rho g L$, while the viscosity is about $0.022 \times \rho g^{1/2} L^{3/2}$ (with $\rho \simeq 1200\,\mathrm{kg\,m^{-3}}$, $g = 9.81\,\mathrm{m\,s^{-2}}$, and $L = 1\,\mathrm{m}$). These values, properly normalized using the different values of the initial radius R_0 of the columns, are also shown in Fig. 3.

Defining the Bingham number $Bi = \overline{\tau_y}/\bar{\eta}$, Bi ranges from 0.014 to 30 for the total of 1020 simulations performed. Their behavior is analyzed in the following.

III. A TYPICAL SLUMP IN THE COURSE OF TIME

Figure 2 shows different snapshots of the evolution of a column of initial aspect ratio $a = 5$ with plastic viscosity $\eta/\rho g^{1/2} R_0^{3/2} = 0.86$ and yield stress $\tau_y/\rho g R_0 = 0.33$. The

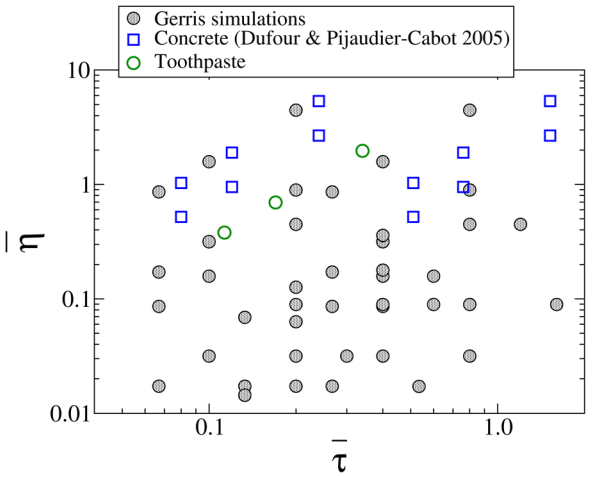

FIG. 3. Combined values of the normalized yield stress $\bar{\tau}_y = \tau_y/(\rho g R_0)$ and normalized plastic viscosity $\bar{\eta}_y = \eta_y/(\rho g^{1/2} R_0^{3/2})$ used in the simulations (black circles); each point coincides with a series of simulations with varying aspect ratio a ($0.2 \leq a \leq 19$). Squares and empty circles coincide with values for concrete and toothpaste, respectively, after proper normalization.

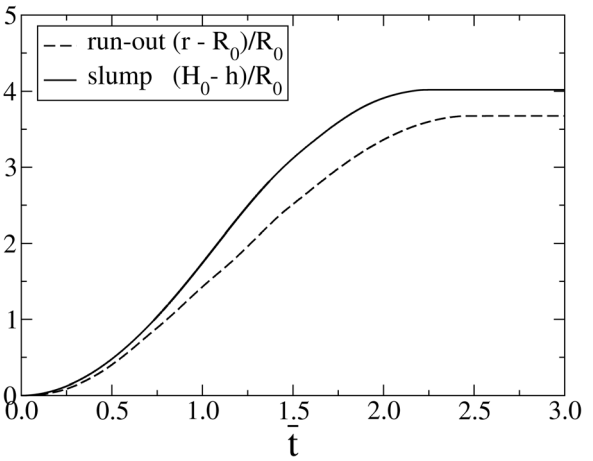

FIG. 4. Evolution of the normalized position of the front $(r - R_0)/R_0$ (or run-out) and of the top of the column $(H_0 - h)/R_0$ (or slump) as a function of the normalized time $\bar{t} = t/\sqrt{H_0/g}$ for the system displayed in Fig. 2.

corresponding time evolution of the position of the front in the course of time $r(t) - R_0$ and of the slump $H_0 - h(t)$ (normalized by R_0) is displayed in Fig. 4. During the flow, the upper-right edge of the column is preserved (due to locally low compressional stress); in the case of very large a, it can be advected downstream. Closer inspection of the state of the spreading layer reveals the existence of areas of higher viscosities (Fig. 5): A "dead" corner is located at the basis of the initial column, and spreads sideways while the flow decelerates and stops; small patches of higher viscosity also appear at the surface of the spreading layer. The preserved edge forms one of them. The inner deformations are made visible in Fig. 6 by mean of passive tracers; we observe maximum stretching in the vicinity of the bottom and in the inner part of the column.

As expected, the typical evolution described above is sensitive to both the rheological parameters and the initial aspect ratio. Larger values of the plastic viscosity η induce smaller run-outs but larger flow durations due to the increase of the time scale related to viscous deformation. Through a different mechanism, larger values of the yield stress induce smaller run-outs and smaller slumping times, the material being quickly frozen in a stress state below the yielding value. Finally, a dependence on the initial aspect ratio a, rather than on H_0 or R_0 alone, is observed, as previously stressed in Sader and Davidson (2005). In particular, for a small initial aspect ratio, depending on the value of the yield stress, no flow may occur at all. All these points are investigated in detail in Sec. IV.

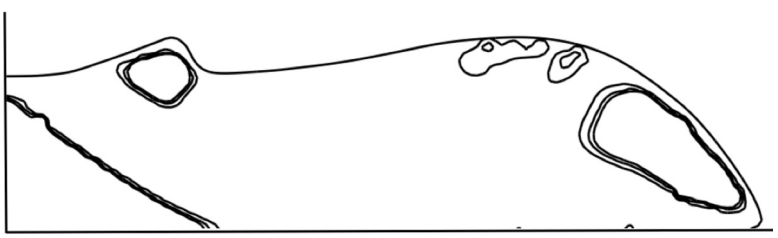

FIG. 5. Snapshot showing areas of maximum viscosity close to flow arrest.

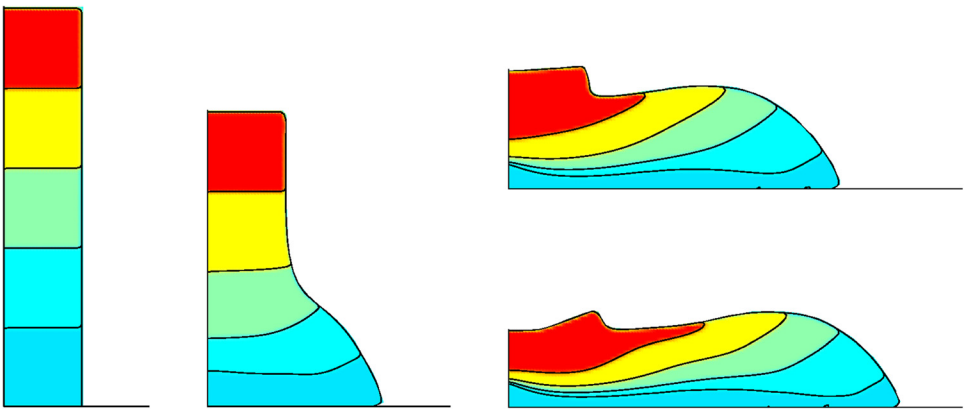

FIG. 6. Snapshots of the slumping shown in Fig. 2 ($a = 5$, $\tau_y/\rho g R_0 = 0.33$, and $\eta/\rho g^{1/2} R_0^{3/2} = 0.86$), at $t/\sqrt{H_0/g} = 0$, 0.85, 1.70, and in the final state, showing inner deformations using VOF tracers.

IV. SCALING LAWS FOR THE SLUMPING AND SPREADING

In the analysis of slumping experiments, it is common practice to use the initial height of the system (H_0) as characteristic length scale against which all other quantities are normalized [Pashias *et al.* (1996); Schowalter and Christensen (1998); Davidson *et al.* (2000); Piau (2005); Roussel and Coussot (2005)]. However, the initial height is not the only length scale affecting the deformation of the column: As demonstrated in Sader and Davidson (2005), its initial radius R_0 plays a major role. The initial height sets the value of the initial compressional stress to be compared with the typical length scale related to the yield stress: $L_y = \tau_y/\rho g$. To single out these two aspects, and prompted by earlier works on slumping of granular matter [Lube *et al.* (2004); Lajeunesse *et al.* (2004); Balmforth and Kerswell (2004); Zenit (2005); Staron and Hinch (2005)], we will use the initial radius R_0 (rather than the initial height H_0) to normalize the slumping and the spreading of the column. Hence, we search for scaling laws relating $(R - R_0)/R_0$ and $(H_0 - H)/R_0$ to $\bar{\tau}_y = \tau_y/\rho g R_0$ and $\bar{\eta} = \eta/\rho g^{1/2} {R_0}^{3/2}$, and to the aspect ratio a.

A. A simple prediction based on equilibrium shape

A simple prediction for the final shape of the slumping material can be obtained by assuming that the final state results from the equilibrium between the pressure induced by the variations of the deposit height and the yield stress [Pashias *et al.* (1996); Roussel *et al.* (2005); Roussel and Coussot (2005)]

$$\rho g h(r) \frac{\partial h(r)}{\partial r} = \tau_y, \tag{2}$$

and by supposing, moreover, that the final shape can be approximated by a cone (or triangle in 2D)

$$h(r) \simeq \frac{H}{R}(R - r). \tag{3}$$

Integrating Eq. (2) between 0 and R gives immediately

$$\tau_y = 2\rho g \frac{H^2}{R}. \tag{4}$$

Since volume conservation implies $HR = 2H_0R_0$, relation (4) leads to the straightforward predictions

$$\frac{R}{R_0} = 2\left(\frac{\rho g R_0}{\tau_y}\right)^{\frac{1}{3}}\left(\frac{H_0}{R_0}\right)^{\frac{2}{3}} = 2\ \bar{\tau}_y{}^{-\frac{1}{3}}\left(\frac{H_0}{R_0}\right)^{\frac{2}{3}}, \tag{5}$$

$$\frac{H}{R_0} = \left(\frac{\tau_y}{\rho g R_0}\right)^{\frac{1}{3}}\left(\frac{H_0}{R_0}\right)^{\frac{1}{3}} = \ \bar{\tau}_y{}^{\frac{1}{3}}\left(\frac{H_0}{R_0}\right)^{\frac{1}{3}} \tag{6}$$

with $\bar{\tau}_y = \tau_y/\rho g R_0$. For large values of the aspect ratio a, the approximation of a cone-shape deformation becomes questionable. Moreover, for small values of the yield stress and large aspect ratios, important spreading and large shear deformations will occur, thus large viscous stresses. We can thus suspect these predictions to be inaccurate in this limit. As a matter of fact, both predictions are poorly supported by the result of the simulations, presented in Secs. IV B and IV C.

B. Scaling law for the run-out as derived from the simulations

An example of the typical dependence of the normalized run-out $(R - R_0)/R_0$ on the initial aspect ratio $a = H_0/R_0$ is displayed in Fig. 7. For small values of a, the stress state remains below the threshold: No flow occurs and $(R - R_0)/R_0 = 0$. For larger values of a, the material spreads and we observe an affine dependence between $(R - R_0)/R_0$ and a

$$\frac{R - R_0}{R_0} = \lambda a - \alpha. \tag{7}$$

Extrapolating this affine dependence allows us for making an estimate of the minimum aspect ratio a_0 characterizing the transition towards sideways spreading: $a_0 = \alpha/\lambda$. Hence, we search for a scaling law for the run-out obeying the shape

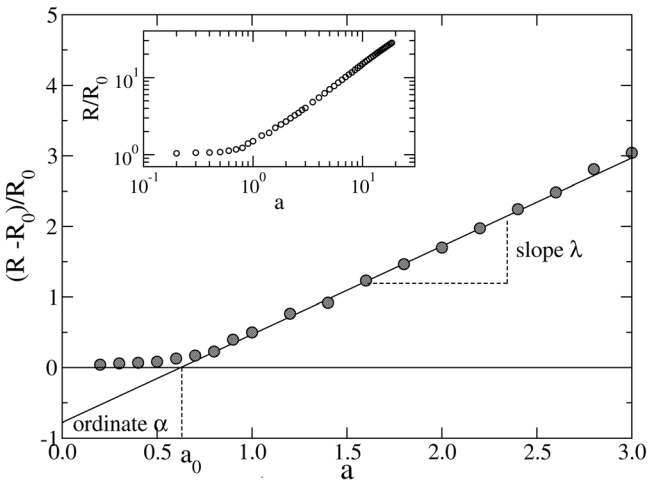

FIG. 7. Typical dependence of the normalized run-out $(R - R_0)/R_0$ on the initial aspect ratio $a = H_0/R_0$, for $\eta/\rho g^{1/2}R_0^{3/2} = 0.86$ and $\tau_y/\rho g R_0 = 0.33$. Inset: R/R_0 as a function of a in log–log scale.

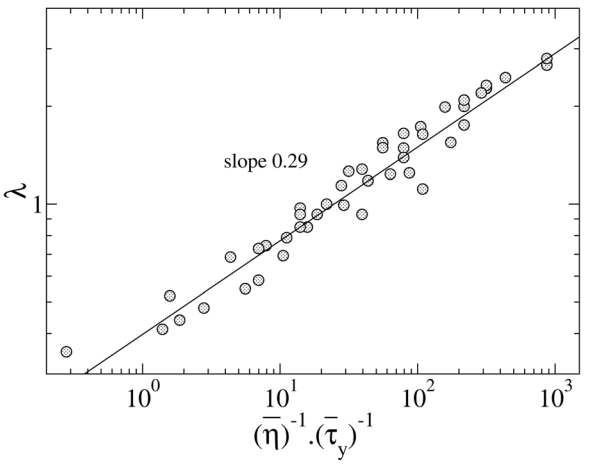

FIG. 8. Scaling laws for the run-out coefficient λ as a function of the normalized yield stress $\bar{\tau}_y$ and plastic viscosity $\bar{\eta}$.

$$\begin{cases} (R - R_0)/R_0 = 0 & \text{if } a < a_0, \\ (R - R_0)/R_0 = \lambda(a - a_0) & \text{if } a \geq a_0. \end{cases} \tag{8}$$

We determine the values of λ and α for all 45 sets of simulations performed, corresponding to different values of $\bar{\eta}$ and $\bar{\tau}_y$. The dependences allowing for the collapse of data following a single master curve are reported in Figs. 8 and 9. The prefactor λ is best approximated by

$$\lambda \simeq 0.40 \left[\frac{1}{\bar{\eta}} \times \frac{1}{\bar{\tau}_y} \right]^{0.29 \pm 0.01} \tag{9}$$

with a correlation coefficient of 0.97 (and $\bar{\tau}_y = \tau_y / \rho g R_0$ and $\bar{\eta} = \eta / \rho g^{1/2} {R_0}^{3/2}$). We observe that both yield stress and plastic viscosity contribute to the sideways spreading with equal weight. We note that the exponent characterizing the dependence on the yield stress is close to the prediction derived in Sec. IV A from mass conservation.

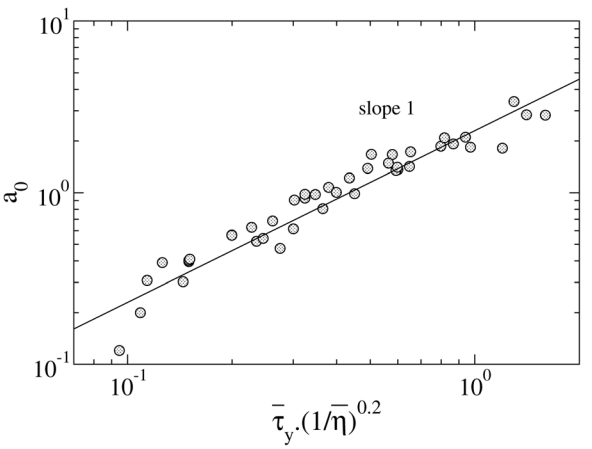

FIG. 9. Scaling laws for the critical aspect ratio a_0 [see Eq. (8)] as a function of the normalized yield stress $\bar{\tau}_y$ and plastic viscosity $\bar{\eta}$.

It is interesting to note that the minimum aspect ratio characterizing the transition towards sideways spreading a_0 does not reflect the slumping behavior. Indeed, a_0 shows the following dependence:

$$a_0 \simeq 2.25\ \bar{\tau}_y \left(\frac{1}{\bar{\eta}}\right)^{0.20 \pm 0.03} \tag{10}$$

with a correlation coefficient of 0.96. It is surprising that a_0 should depend on the plastic viscosity, moreover, following an inverse correlation: Indeed, we expect a small viscosity to favor slumping. Yet consistently, in the range of parameters studied, we observe that a large viscosity associated with a small yield stress (that is, a small Bingham number $B_i = \bar{\tau}_y/\bar{\eta}$) implies a smaller offset in the dependence between run-out and initial aspect ratio. The fact that no sideways spreading is detected does not mean, however, that no slumping occurs. Indeed, depending on the value of τ_y, a low plastic viscosity may result in squat columns flanks to deform and create a sideways swell, without the base of the column to actually move. In that case, however, slumping occurs. Hence, the critical aspect ratio characterizing the transition to slumping must be estimated from the direct evaluation of the final height H.

C. Scaling law for the slumping as derived from the simulations

Using the same set of simulations as shown in Fig. 7, the normalized slump $(H_0 - H)/R_0$ as a function of the initial aspect ratio $a = H_0/R_0$ is shown in Fig. 10. For small a, no slump occurs and $(H_0 - H)/R_0 = 0$. For larger a, we observe an affine dependence

$$\frac{H_0 - H}{R_0} = \lambda' a - \alpha', \tag{11}$$

as exhibited by the run-out [see Eq. (7)]. However, in this case, seemingly irrespective of the value of $\bar{\eta}$ or $\bar{\tau}_y$, the slope is constant and equal to one: $\lambda' \simeq 1$. In other words, the effect of the initial aspect ratio a on the final height H is negligible. Hence, relation (11) is equivalent to

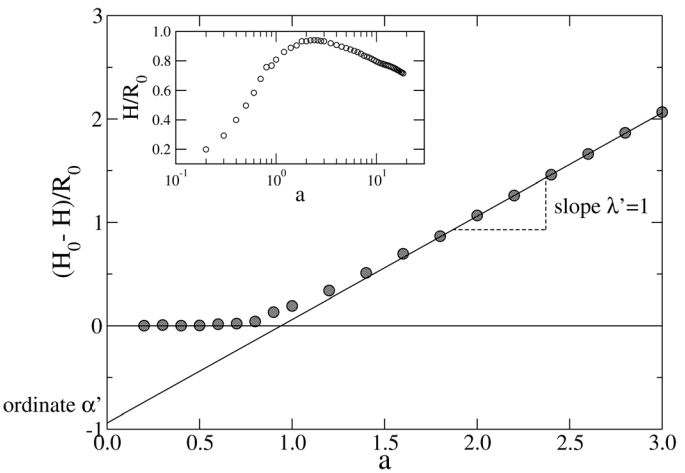

FIG. 10. Typical dependence of the normalized slump $(H_0 - H)/R_0$ as a function of the initial aspect ratio $a = H_0/R_0$, for $\eta/\rho g^{1/2} R_0^{3/2} = 0.86$ and $\tau_y/\rho g R_0 = 0.33$. Inset: The normalized final height H/R_0 as a function of a in linear–log scale.

$$\frac{H}{R_0} \simeq \alpha'. \tag{12}$$

As precedently, α' is determined for all 45 sets of simulations corresponding to different values of $\overline{\tau_y}$ and $\bar{\eta}$ (shown in Fig. 3). The resulting dependence is reported in Fig. 11, and is best approximated by

$$\frac{H}{R_0} \simeq 3.01 \left(\frac{\tau_y}{\rho g R_0}\right)^{0.66 \pm 0.03} = 3.01\, \bar{\tau}_y^{0.66 \pm 0.03} \tag{13}$$

with a correlation coefficient of 0.95. The final height of the collapsed column is thus independent of the initial height, presumably due to the absence of large inertial effects. Moreover, it is not affected by the value of the plastic viscosity $\bar{\eta}$, as generally assumed in numerical studies [Tattersall and Banfill (1983); Schowalter and Christensen (1998); Sader and Davidson (2005); Roussel and Coussot (2005)] and theoretical derivations [Chamberlain *et al*. (2004)].

Using Eqs. (11) and (13), we can write

$$\begin{cases} (H_0 - H)/R_0 = 0 & \text{if } a < a_c, \\ (H_0 - H)/R_0 = (a - a_c) & \text{if } a \geq a_c, \\ a_c = 3.01\, \bar{\tau}_y^{0.66}, \end{cases} \tag{14}$$

where a_c is the critical aspect ratio characterizing the transition to slumping.

This result is qualitatively in agreement with the result of Sader and Davidson (2005), where a polynomial relation between $\rho g R_0/(2\tau_y)$ and $1/a_c$ was observed for axisymmetric columns: We find that a polynomial relation (although of a different order) is acceptable for the same range of $\bar{\tau}_y$ (see Fig. 12). Differences between the two approaches include the geometry [axisymmetric in Sader and Davidson (2005) vs planar in the present contribution] and the values of the plastic viscosity [equal to zero in Sader and Davidson (2005) while varied over 2 orders of magnitude in the present contribution]; yet, the dependences found to involve the same parameters, namely yield stress and critical aspect ratio, following the same trend.

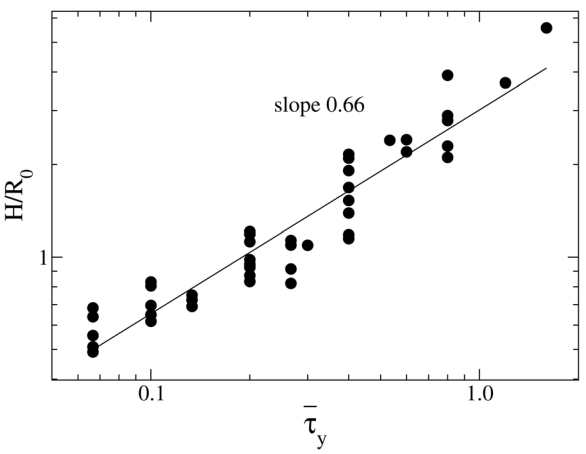

FIG. 11. Scaling law for the final normalized height H/H_0 as a function of the normalized yield stress $\bar{\tau}_y = \tau_y/\rho g R_0$.

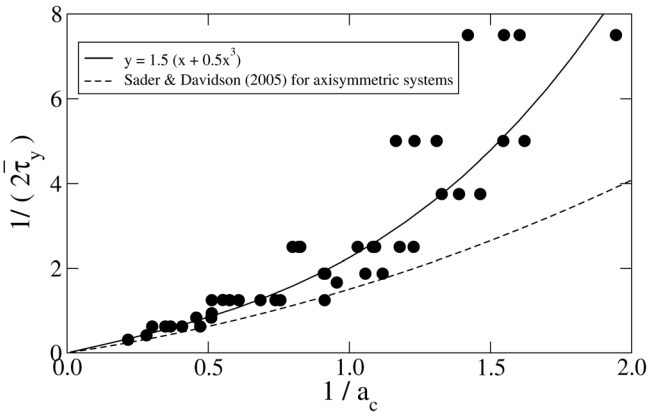

FIG. 12. Comparison with the results of Sader and Davidson (2005) for axisymmetric columns with zero viscosity: $1/2\bar{\tau}_y \simeq 1/a_c + 0.5(1/a_c)^2 + 0.005(1/a_c)^4$. We find in 2D $1/2\bar{\tau}_y \simeq 1.5(1/a_c + 0.5(1/a_c)^3)$.

By contrast, our results are not fully compatible with the theoretical prediction of Pashias *et al.* (1996), also discussed in Schowalter and Christensen (1998), Davidson *et al.* (2000), and Roussel and Coussot (2005). Indeed, the theoretical derivation in Pashias *et al.* (1996) leads to the following prediction for the slump:

$$\frac{H_0 - H}{H_0} = 1 - 2\frac{\tau_y}{\rho g H_0}\left(1 - \ln\left(2\frac{\tau_y}{\rho g H_0}\right)\right). \tag{15}$$

Rewritten in term of final height H and normalized according to the choice adopted in the present contribution, Eq. (15) is equivalent to

$$\frac{H}{R_0} = 2\bar{\tau}_y(1 - \ln(2\bar{\tau}_y a)) \tag{16}$$

with $\bar{\tau}_y = \tau_y/\rho g R_0$. While our simulations suggest that H/R_0 is only dependent on $\bar{\tau}_y$ [scaling (13)], the prediction of Pashias *et al.* (1996) implies an additional dependence on the aspect ratio a. In other words, it combines the effect of both rheological properties and geometry, i.e., compressional stress. This is illustrated in Fig. 13, where we have reported $(H_0 - H)/H_0$ as a function of $\tau_y/\rho g H_0$ for two distinct values of the yield stress τ_y, i.e., corresponding to two different materials. For each value of τ_y (i.e., for each material), the aspect ratio a varies, while R_0 and $\bar{\eta}$ are kept constant. In the case $\tau_y = 0.01\rho g L$ (where $L = 1$ m is an arbitrary length scale not related to the system geometry), we observe that our data points nicely match prediction (16); this is, however, a purely geometrical effect due to the representation in terms of $\tau_y/\rho g H_0$. Indeed, varying a implies varying H_0 and thus varying the ratio $\tau_y/\rho g H_0$ although τ_y is constant: In this precise case, we verify Eq. (15), while actually not probing the material property.

If we look at the case $\tau_y = 0.04\rho g L$ (where $L = 1$ m), we observe a systematic shift compared to the case $\tau_y = 0.01\rho g L$, that is, our data do not collapse following Eq. (15); yet, it is still compatible in shape with Eq. (15). Here again, only the geometry (i.e., the variations of a) is responsible for the relative agreement with prediction (15), without involving any meaning in terms of the material rheological properties.

This result prompts a comment on the importance of the normalization choice. By using the initial height, one mixes the effect of compressional stress and rheology. While

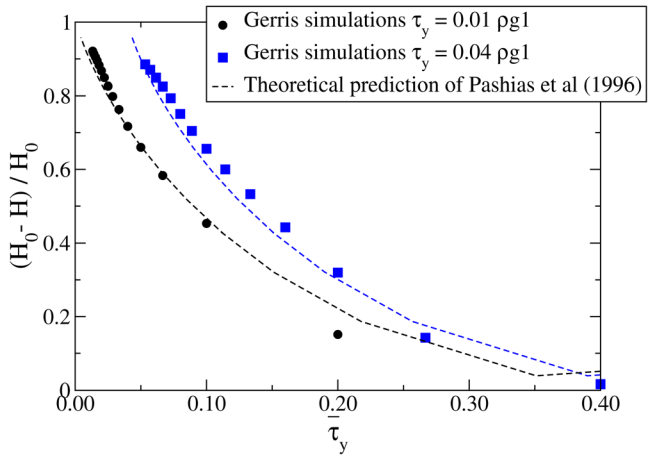

FIG. 13. Comparison with the results of Pashias *et al.* (1996): Slump normalized by the initial height $(H_0 - H)/H_0$ as a function of the normalized yield stress $\bar{\tau}_y = \tau_y/\rho g H_0$ for two series of simulations corresponding to two given materials (i.e., two given values of $\tau_y/\rho g L$, $L = 1$ m), and theoretical prediction from Pashias *et al.* (1996) [see Eq. (15)]. The agreement reflects geometrical constraints only.

this is common practice to define such nondimensional numbers where the behavior of the system is well described by an equation (as Newtonian fluids, for instance), it is not straightforward when the behavior of the system regarding all independent parameters is far from fully understood, as for the Bingham slump. As a result, one can easily mistake the effect of geometry for those of material, thus allowing for incorrect interpretation. This is particularly likely to happen in experiments where the yield stress of materials used varies over a relatively small interval, while geometry can be changed at command.

V. DISCUSSION

A. Comparison with the slumping of granular material

Granular materials and Bingham plastics share an important rheological property: They behave like a solid at low shear stress and like a fluid at higher shear stress. However, the threshold marking the transition between one and the other state is of a different nature. While in Bingham plastics, the threshold is given by an absolute yield value τ_y, the threshold in granular matter is given by frictional properties, and thus depends locally on the compressional stress: $\tau_y = \mu P$, where μ is the coefficient of friction and P the pressure. Moreover, granular flows exhibit shear thickening properties. It is interesting to observe how these differences reflect on the slumping dynamics and the corresponding scaling laws. In Lajeunesse *et al.* (2004), Lube *et al.* (2004), Balmforth and Kerswell (2004), and Staron and Hinch (2005), for instance, the collapse of granular material was investigated experimentally (using sand, rice, and glass beads) and numerically (applying the discrete contact dynamics method), following the same set-up as applied in this paper. The scaling laws thus obtained in 2D read

$$\frac{R - R_0}{R_0} = \lambda(\mu) \times a^{\alpha}, \quad a \geq a_c, \tag{17}$$

$$\frac{H}{R_0} = \lambda'(\mu) \times a^{\alpha'}, \quad a \geq a'_c \tag{18}$$

with $\alpha \simeq 0.67$ and $\alpha' \in [0.3, 0.4]$ depending on the authors, and where a_c and a'_c are critical values of the aspect ratio, varying from 0.7 to 2.8 depending on the authors. The prefactors λ and λ' are functions of the coefficient of friction μ only.

The difference between these scalings and those obtained from the present simulations—that is relations (9) and (13)—is manifest. However, they might not be incompatible. Indeed, the yield stress for granular columns is given by $\tau_y = \mu\rho g H_0$. Replacing this in Eq. (13) gives immediately $H/R_0 = \lambda'(\mu)\, a^{0.66}$, where $\lambda'(\mu) = 3.01\, \mu^{0.66}$, thus becoming similar in shape to Eq. (18). In the same way, replacing $\tau_y = \mu\rho g H_0$ in Eq. (9) leads directly to $(R - R_0)/R_0 \propto \lambda(\mu)\, a^{0.71}$, where $\lambda(\mu) = 4.0\, \mu^{-0.29}$ [a trend compatible with numerical observations in Staron and Hinch (2007)], thus sharing similarities with Eq. (17).

Viscous terms are more intricate. In dry granular flows, the viscosity can be approximated by $\eta = \mu P/|\dot{\gamma}|$, where $\dot{\gamma}$ is the shear rate [Jop *et al.* (2006); Lagrée *et al.* (2011)]. There are no obvious scales for the pressure and the shear rate during the sideways spreading. Note, however, that the choice of $P = \rho g R_0$ and $|\dot{\gamma}| = \sqrt{g/R_0}$ leads immediately to the following relation between friction and viscosity: $\mu = \eta/\rho g^{\frac{1}{2}} R_0^{\frac{3}{2}}$, and can thus be replaced in scaling (9). This is certainly too speculative to draw any conclusion on the viscous behavior of granular slump experiments. But we can nevertheless conclude that Bingham and granular scalings may be less different than they appear at first. Granular matter forms an example of viscoplastic behavior where yield stress and viscosity are not independent, but are coupled (here through internal friction properties). We may question the existence of such coupling in other common materials, like mud or fresh concrete.

B. About cement and concrete

Granular matter forms an example of viscoplastic behavior where yield stress and viscosity are coupled. It would be interesting to establish whether such a coupling exists in real Binghamlike materials, and among them concrete. Indeed, unlike the ideal Bingham material simulated in this paper, viscosity and yield stress in fresh concrete are not necessarily independent quantities. For instance, the data given in Dufour and Pijaudier-Cabot (2005) for three different model concretes suggest that plastic viscosity and yield stress are related quantities: The greater the viscosity, the greater the yield stress.

From the systematic analysis of the simulations, the final slump height appears to be essentially independent of the viscosity, but to scale like $(\tau_y/\rho g R_0)^{0.66}$. This brings the conclusion that slumping tests, such as the Abram cone widely used to measure the properties of fresh concrete, do give information on the yield stress, but little on the viscosity. Clarifying the relation between these two quantities might contribute to a more reliable calibration of slump tests as *in situ* measurements of rheological parameters. In this perspective, the present study suggests that sideways spreading rather than slumping keeps the signature of the viscous behavior.

VI. CONCLUSION

Applying the Gerris Navier–Stokes solver allowing for the modeling of biphasic mixtures using a VOF method, we simulate the collapse of columns of Bingham plastics under gravity in 2D. The rheological properties of the material—plastic viscosity and yield stress—as well as the geometry of the columns—initial radius and initial height—were varied independently. The final slumping height and final run-out were measured and scaling laws were derived. Our results show that the run-out R increases linearly with the initial height of the column H_0, with a prefactor depending inversely on both plastic viscosity and yield stress

$$\begin{cases} (R - R_0)/R_0 = 0 & \text{if } a < a_0, \\ (R - R_0)/R_0 = \lambda(a - a_0) & \text{if } a \geq a_0, \\ \lambda \simeq 0.40 \left[\dfrac{1}{\bar{\eta}} \times \dfrac{1}{\bar{\tau}_y}\right]^{0.29 \pm 0.01}, \\ a_0 \simeq 2.25\ \bar{\tau}_y \left(\dfrac{1}{\bar{\eta}}\right)^{0.20}, \end{cases} \tag{19}$$

where $a = H_0/R_0$ is comprised in the interval [0.2, 19], $\bar{\tau}_y = \tau_y/\rho g R_0$ is comprised in the interval [0.06, 1.6], and $\bar{\eta} = \eta/\rho g^{1/2} {R_0}^{3/2}$ is comprised in the interval [0.01, 5].

By contrast, we find that the final height H is essentially insensitive to plastic viscosity and depends on the value of the yield stress. We find no effect of the initial height of the column, whereby we conclude that inertial effects are negligible. We derive the transition to slumping following the scaling:

$$\begin{cases} (H_0 - H)/R_0 = 0 & \text{if } a < a_c, \\ (H_0 - H)/R_0 = (a - a_c) & \text{if } a \geq a_c, \\ a_c \simeq 3.01\ \bar{\tau}_y^{0.66}, \end{cases} \tag{20}$$

where $a = H_0/R_0$ is comprised in the interval [0.2, 19] and $\bar{\tau}_y = \tau_y/\rho g R_0$ is comprised in the interval [0.06, 1.6]. This last result is compatible with the conclusions of Sader and Davidson (2005) relative to the slump in axisymmetric configuration. When compared with the theoretical prediction of Pashias *et al*. (1996), we find a partial agreement which, however, only reflects the geometrical constraints imposed by varying the aspect ratio. This result shows the importance of the normalization choice. By using the initial height, one mixes the effect of compressional stress, geometry, and rheology in one single nondimensional parameter. While this is common practice to define such nondimensional numbers where the behavior of the system is well described by an equation (as Newtonian fluids, for instance), it is not straightforward when the behavior of the system regarding all independent parameters is far from fully understood, as for the Bingham slump. As a result, one can easily mistake the effect of geometry for those of the material properties, thus allowing for incorrect interpretation. This is particularly likely to happen in experimental settings where the yield stress of materials used varies over a relatively small interval, while geometry can be changed at command.

The scaling laws discussed in this contribution were obtained for 2D configurations; an interesting step for practical application would be to investigate how the scalings are modified in the axisymmetric case, as studied by Sader and Davidson (2005). This aspect will be addressed in future work.

ACKNOWLEDGMENT

The first author acknowledges funding by the REA Marie Curie Action Grant GEOGRAF No. 297843.

References

Balmforth, N. J., and R. R. Kerswell, "Granular collapse in two dimensions," J. Fluid Mech. **538**, 399–428 (2005).

Balmforth, N. J., R. V. Craster, P. Peronac, A. C. Rustd, and R. Sassie, "Viscoplastic dam breaks and the Bostwick consistometer," J. Non-Newtonian Fluid Mech. **142**(1–3), 63–78 (2007).

Bird, R. B., R. C. Armstrong, and O. Hassager, *Dynamics of Polymeric Liquids*, 2nd ed. (Wiley-Interscience, New York, 1987).

Chamberlain, J. A., D. J. Horrobin, K. A. Landman, and J. E. Sader, "Upper and lower bounds for incipient failure in a body under gravitational loading," J. Appl. Mech. **71**, 586–589 (2004).

Davidson, M. R., N. H. Khan, and Y. L. Yeow, "Collapse of a cylinder of a Bingham fluid," ANZIAM J. **42**(E), C499–C517 (2000).

Dubash, N., N. J. Balmforth, A. C. Slima, and S. Cochard, "What is the final shape of a viscoplastic slump?," J. Non-Newtonian Fluid Mech. **158**(13), 91–100 (2009).

Dufour, F., and G. Pijaudier-Cabot, "Numerical modelling of concrete flow: Homogeneous approach," Int. J. Numer. Analyt. Meth. Geomech. **29**(4), 395–416 (2005).

Ferraris, C. F., and F. de Larrard, "Modified slump test to measure rheological parameters of fresh concrete," Cem., Concr., Aggregates **20**(2), 241–247 (1998).

Hogg, A. J., and G. P. Matson, "Slumps of viscoplastic fluids on slopes," J. Non-Newtonian Fluid Mech. **158**(13), 101–112 (2009).

Jop, P., Y. Forterre, and O. Pouliquen, "A rheology for dense granular flows," Nature **441**, 727–730 (2006).

Lagrée, P.-Y., L. Staron, and S. Popinet, "The granular column collapse as a continuum: Validity of a two-dimensional Navier–Stokes model with a μ(I)-rheology," J. Fluid Mech. **686**, 378–408 (2011).

Lajeunesse, E., A. Mangeney-Castelneau, and J.-P. Vilotte, "Spreading of a granular mass on an horizontal plane," Phys. Fluids **16**, 2371–2381 (2004).

Lube, G., H. E. Huppert, R. S. J. Sparks, and M. A. Hallworth, "Axisymmetric collapses of granular columns," J. Fluid Mech. **508**, 175–199 (2004).

Pashias, N., D. V. Boger, J. Summers, and D. J. Glenister, "A fifty cent rheometer for yield stress measurement," J. Rheol. **40**(6), 1179–1189 (1996).

Piau, J.-M., "Axisymmetric slump and spreading of cohesive plastic soft materials: A yield stress measurement by consisto-rheometry," J. Rheol. **49**, 1253–1276 (2005).

Popinet, S., "Gerris: A tree-based adaptive solver for the incompressible Euler equations in complex geometries," J. Comput. Phys. **190**(2), 572–600 (2003).

Popinet, S., "An accurate adaptive solver for surface-tension-driven interfacial flows," J. Comput. Phys. **228**, 5838–5866 (2009).

Roussel, N., C. Stefani, and R. Leroy, "From mini-cone test to Abrams cone test: Measurement of cement-based materials yield stress using slump tests," Cem. Concr. Res. **35**(5), 817–822 (2005).

Roussel, N., and P. Coussot, ""Fifty-cent rheometer" for yield stress measurements: From slump to spreading flow," J. Rheol. **49**, 705–718 (2005).

Sader, J. E., and M. R. Davidson, "Scaling behavior for gravity induced flow of a yield stress material," J. Rheol. **49**, 105–112 (2005).

Scardovelli, R., and S. Zaleski, "Direct numerical simulation of free-surface and interfacial flow," Annu. Rev. Fluid Mech. **31**, 567–603 (1999).

Schowalter, W. R., and G. Christensen, "Toward a rationalization of the slump test for fresh concrete: Comparisons of calculations and experiments," J. Rheol. **42**, 865–870 (1998).

Staron, L., and E. J. Hinch, "Study of the collapse of granular columns using 2D discrete-grains simulation," J. Fluid Mech. **545**, 1–27 (2005).

Staron, L., and E. J. Hinch, "The spreading of a granular mass: Role of grain properties and initial conditions," Granular Matter **9**, 205–217 (2007).

Staron, L., P.-Y. Lagrée, and S. Popinet, "The granular silo as a continuum plastic flow: The hour-glass vs the clepsydra," Phys. Fluids **24**(10), 103301 (2012).

Tallarico, A., and M. Dragoni, "A three-dimensional Bingham model for channeled lava flows," J. Geophys. Res. **105**(B11), 25969–25980, doi:10.1029/2000JB900201 (2000).

Tattersall, G. H., and P. G. F. Banfill, *The Rheology of Fresh Concrete* (Pitman Advanced Publishing Program, 1983).

Whipple, K. X., "Open-channel flow of Bingham fluids: Applications in debris-flow research," J. Geol. **105**(2), 243–262 (1997).

Zenit, R., "Computer simulations of the collapse of a granular column," Phys. Fluids **17**, 031703 (2005).